Transient oxidative stress damages mitochondrial machinery inducing persistent beta-cell dysfunction

Li, Ning; Brun, Thierry; Cnop, Miriam; Cunha, Daniel A.; Eizirik, Decio L.; Maechler, Pierre

THE JOURNAL OF BIOLOGICAL CHEMISTRY VOL. 284, NO. 35, pp. 23602–23612, August 28, 2009

Transient Oxidative Stress Damages Mitochondrial Machinery Inducing Persistent β-Cell Dysfunction*[S]

Received for publication, March 10, 2009, and in revised form, May 22, 2009 Published, JBC Papers in Press, June 22, 2009, DOI 10.1074/jbc.M109.024323

Ning Li[‡1], Thierry Brun[‡1], Miriam Cnop[§¶], Daniel A. Cunha[§], Decio L. Eizirik[§], and Pierre Maechler[‡1,2]

From the [‡]Department of Cell Physiology and Metabolism, Faculty of Medicine, University of Geneva, rue Michel-Servet 1, CH-1211 Geneva 4, Switzerland and the [§]Laboratory of Experimental Medicine and [¶]Division of Endocrinology, Erasmus Hospital, Université Libre de Bruxelles, Route de Lennik, 808 CP-618, Brussels 1070, Belgium

Transient exposure of β-cells to oxidative stress interrupts the transduction of signals normally coupling glucose metabolism to insulin secretion. We investigated putative persistence of effects induced by one transient oxidative stress (200 μM H_2O_2, 10 min) on insulin secreting cells following recovery periods of days and weeks. Three days after oxidative stress INS-1E cells and rat islets exhibited persistent dysfunction. In particular, the secretory response to 15 mM glucose was reduced by 40% in INS-1E cells stressed 3 days before compared with naïve cells. Compared with non-stressed INS-1E cells, we observed reduced oxygen consumption (−43%) and impaired glucose-induced ATP generation (−46%). These parameters correlated with increased mitochondrial reactive oxygen species formation (+60%) accompanied with down-regulation of subunits of the respiratory chain and decreased expression of genes responsible for mitochondrial biogenesis (*TFAM*, −24%; *PGC-1α*, −67%). Three weeks after single oxidative stress, both mitochondrial respiration and secretory responses were recovered. Moreover, such recovered INS-1E cells exhibited partial resistance to a second transient oxidative stress and up-regulation of UCP2 (+78%) compared with naïve cells. In conclusion, one acute oxidative stress induces β-cell dysfunction lasting over days, explained by persistent damages in mitochondrial components.

Pancreatic β-cells are poised to sense blood glucose to regulate insulin exocytosis and thereby glucose homeostasis. The conversion from metabolic signals to secretory responses is mediated through mitochondrial metabolism (1). Failure of the insulin secreting β-cells, a common characteristic of both type 1 and type 2 diabetes, derives from various origins, among them mitochondrial impairment secondary to oxidative stress is a proposed mechanism (2).

Oxidative stress is characterized by a persistent imbalance between excessive production of reactive oxygen species (ROS)[3] and limited antioxidant defenses. Examples of ROS include superoxide ($O_2^{\cdot-}$), hydroxyl radical ($OH^{\cdot}$), and hydrogen peroxide (H_2O_2). Superoxide can be converted to less reactive H_2O_2 by superoxide dismutase (SOD) and then to oxygen and water by catalase (CAT), glutathione peroxidase (GPx), and peroxiredoxin, which constitute antioxidant defenses. Increased oxidative stress and free radical damages have been proposed to participate in the diabetic state (3). In type 1 diabetes, ROS are implicated in β-cell dysfunction caused by autoimmune reactions and inflammatory cytokines (4). In the context of type 2 diabetes, excessive ROS could promote deficient insulin synthesis (5, 6) and apoptotic pathways in β-cells (5, 7). Of note, ROS fluctuations may also contribute to physiological control of cell functions (8), including the control of insulin secretion (9). It should also be stressed that metabolism of physiological nutrient increases ROS without causing deleterious effects on cell function. However, uncontrolled increase of oxidants, or reduction of their detoxification, leads to free radical-mediated chain reactions ultimately triggering pathogenic events. Pancreatic β-cells are relatively weak in expressing free radical-quenching enzymes SOD, CAT, and GPx (10, 11), rendering those cells particularly susceptible to oxidative attacks (12). Mitochondria are not only the main source of cellular oxidants, they are also the primary target of ROS (13, 14).

Mitochondria are essential for pancreatic β-cell function, and damages to these organelles are well known to markedly alter glucose-stimulated insulin secretion (15). The mitochondrial genome constitutes one of the targets, encoding for 13 polypeptides essential for the integrity of electron transport chain (16). Damages to mitochondrial DNA (mtDNA) induce mutations that in turn may favor ROS generation, although the contribution of mtDNA mutations to ROS generation remains unclear. We previously reported that patient-derived mitochondrial A3243G mutation, causing mitochondrial inherited diabetes, is responsible for defective mitochondrial metabolism associated with elevated ROS levels and reduced antioxidant enzyme expression (17). On the other hand, mtDNA mutator mice exhibit accelerated aging without changes in superoxide

* This work was supported in part by the Swiss National Science Foundation (to P. M.), the European Foundation for the Study of Diabetes (EFSD) through an EFSD fellowship supported by Bristol-Myers Squibb Company (to N. L.), a fellowship from the Hans Wilsdorf Foundation, Geneva, Switzerland (to N. L.), the Research Foundation of the European Association for the study of Diabetes, the European Union Integrated Project EuroDia LSHM-CT-2006-518153 in the Framework Programme 6 of the European Community (to M. C. and D. L. E.), and the Belgium Fonds National de la Recherche Scientifique-Recherche Scientifique Medicale (to M. C. and D. L. E.).

[S] The on-line version of this article (available at http://www.jbc.org) contains supplemental Figs. S1–S4 and Tables S1–S3.

[1] Members of the Geneva Programme for Metabolic Disorders.

[2] To whom correspondence should be addressed: Dept. of Cell Physiology and Metabolism, University Medical Centre, rue Michel-Servet 1, 1211 Geneva 4, Switzerland. Tel.: 41-22-379-5554; Fax: 41-22-379-5543; E-mail: Pierre.Maechler@unige.ch.

[3] The abbreviations used are: ROS, reactive oxygen species; SOD, superoxide dismutase; CAT, catalase; GPx, glutathione peroxidase; mtDNA, mitochondrial DNA; BSA, bovine serum albumin; FCCP, carbonyl cyanide *p*-trifluoromethoxyphenylhydrazone; PBS, phosphate-buffered saline; TUNEL, terminal deoxynucleotidyl transferase-mediated dUTP nick end labeling; BrdUrd, bromodeoxyuridine; $\Delta\Psi_m$, mitochondrial membrane potential.

levels in embryonic fibroblasts (18), showing that ROS generation can be dissociated from mtDNA mutations.

In humans, mitochondrial defects typically appear with aging (19), accompanied by sustained ROS generation and progressive oxidant-induced damages (20). In support of this "mitochondrial theory of aging" (21), accumulating evidence shows that in older individuals mitochondria are altered, both morphologically and functionally (22). These age-related mitochondrial changes are foreseen to play a role in the late onset diabetes. In a rat model of intrauterine growth retardation, a vicious cycle between accumulation of mtDNA mutations and elevation of ROS production has been associated to β-cell abnormalities and the onset of type 2 diabetes in adulthood (23). Similarly, mitochondrion-derived ROS impair β-cell function in the Zucker diabetic fatty rat (24). Altogether, these observations point to ROS action as a triggering event inducing mitochondrial dysfunction and ultimately resulting in the loss of the secretory response in β-cells (14).

In vitro, oxidative stress applied to β-cells rapidly interrupts the transduction of signals normally coupling glucose metabolism to insulin secretion (12, 25). Specifically, we reported that INS-1E β-cells and rat islets subjected to a 10-min H_2O_2 exposure exhibit impaired secretory response associated with mitochondrial dysfunction appearing already during the first minutes of oxidative stress (12). In the context of the mitochondrial theory of aging (21, 26), it is important to know whether transient exposure to H_2O_2 could possibly induce persistent modifications of mitochondrial function. Cells surviving an oxidative stress might carry defects leading to progressive loss of β-cell function. In the present study, we asked the simple but unanswered question if a short transient oxidative stress could induce durable alterations of the mitochondria and thereby chronically impair β-cell function. INS-1E β-cells and rat islets were transiently exposed to H_2O_2 for 10 min and analyzed after days and weeks of standard tissue culture.

EXPERIMENTAL PROCEDURES

Cell Culture and Treatments—INS-1E cells were used as a well differentiated clone derived from rat insulinoma INS-1 cells and cultured as detailed previously (26). Pancreatic islets were isolated by collagenase digestion from Wistar rats weighting 200–250 g, hand-picked and cultured free-floating in RPMI 1640 medium before experiments (27).

INS-1E cells were seeded in Falcon (OmniLab, Mettmenstetten, Switzerland) multiwell plates and Petri dishes treated with polyornithine (Sigma-Aldrich). After 2 days of culture, cells were exposed to 200 μM H_2O_2 (Sigma-Aldrich) and 10 min later 100 units/ml CAT (Sigma-Aldrich) were added to neutralize H_2O_2. The 200 μM concentration of H_2O_2 was selected according to: (i) the dose-response performed previously showing direct effects above 100 μM (12); (ii) the dose-response performed on INS-1E cells analyzed 3 days after the 10-min oxidative stress (see supplemental Figs. S1 and S2). Following the H_2O_2 and CAT treatment, cells were further cultured in normal complete media and, where indicated, passaged once a week until analysis. Control cells were cultured for the same period of time as stressed cells. Regarding primary cells, rat pancreatic islets were isolated, exposed to oxidative stress as described above, and cultured before hand-picking for analyses.

Insulin Secretion Assay—Insulin secretion assay was performed as detailed previously (26). In brief, cells were preincubated in glucose-free Krebs-Ringer bicarbonate HEPES buffer (KRBH, in mM: 135 NaCl, 3.6 KCl, 5 $NaHCO_3$, 0.5 NaH_2PO_4, 0.5 $MgCl_2$, 1.5 $CaCl_2$, 10 HEPES, pH 7.4) containing 0.1% bovine serum albumin (KRBH/BSA). Next, cells were incubated for 30 min at 37 °C in KRBH/BSA containing basal 2.5 mM or stimulatory 15 mM glucose concentrations. Non-nutrient-stimulated secretion was induced by 30 mM KCl (at 2.5 mM glucose).

Cultured rat islets were hand-picked for either static insulin secretion or perifusion experiments. For perifusion protocols, cultured islets were placed by 10 in chambers of 250-μl volume (Brandel, Gaithersburg, MD), and then perifused at a flow rate of 1 ml/min (27) with KRBH/BSA medium containing sequentially basal 2.8 mM glucose followed by stimulatory 16.7 mM glucose. Insulin was collected, and insulin levels were determined by radioimmunoassay (Linco, St. Charles, MO).

$\Delta\Psi_m$ and ATP Levels—The mitochondrial membrane potential ($\Delta\Psi_m$) was measured as described (26) in INS-1E cells loaded with Rhodamine-123 (Molecular Probes, Eugene, OR) and monitored in a plate-reader fluorometer (Fluostar Optima, BMG Lab Technologies, Offenburg, Germany). At indicated time points, glucose was raised to 15 mM, and then 1 μM of the protonophore carbonyl cyanide *p*-trifluoromethoxyphenylhydrazone (FCCP, Sigma-Aldrich) was added.

Cellular ATP levels were monitored in cells expressing the ATP-sensitive bioluminescent probe luciferase after transduction with the viral construct AdCAG-Luc the day before measurements (28, 29). In the presence of 100 μM luciferin, cells were stimulated with 15 mM glucose and 2 mM NaN_3 was added at the end as a mitochondrial poison. Luminescence was monitored in a plate-reader luminometer (26). Total cellular ATP concentrations were determined according to manufacturer's instructions (ATP Bioluminescence Assay Kit HS II, Roche Applied Science) following cell incubation for 10 min with KRBH at 2.5 mM and 15 mM glucose.

Oxygen Consumption—Oxygen consumption measurements were performed either on live cell suspension or isolated mitochondria. At indicated times cells were trypsinized and left to recover (60 min, 37 °C) before stimulation with 15 mM glucose. For isolated mitochondria, INS-1E cells were washed with PBS, scraped, collected in mitochondria isolation buffer (250 mM sucrose, 20 mM Tris/HCl, and 2 mM EGTA at pH 7.4) supplemented with 0.5% BSA, and pelleted by centrifugation (10 min at 1000 rpm). Pellets were then resuspended with mitochondria isolation buffer and homogenized in a 3-ml Teflon glass potter with 500 rpm rotation rate for 20 up-and-down strokes, followed by centrifugation for 8 min at 1500 × *g* to pull down nuclei. Supernatants were centrifuged for 10 min at 12,000 × *g*, and the resulting pellets were collected with respiration buffer (200 mM sucrose, 50 mM KCl, 20 mM Tris/HCl, 1 mM $MgCl_2$, and 5 mM KH_2PO_4 at pH 7.0). After protein determination, 100 μg of mitochondria were used for measurements of oxygen consumption using a Clark-type electrode (Rank Brothers Ltd., Cambridge, UK). Succinate (5 mM) and 150 μM ADP-induced

oxygen consumptions were performed on intact mitochondria directly after isolation. Oxygen consumption induced by NADH (5 mM) was measured in permeabilized mitochondria following snap-freezing in liquid nitrogen and thawing four times. This procedure weakened mitochondrial membrane shortly before experiments and thereby permitted uncoupled respiration measurements.

Complex I Activity and Mitochondrial ROS Generation—Complex I activity was measured as the rate of NADH-driven electron flux through complex I using a variation of the Amplex Red assay (Molecular Probes), which detects mitochondrial H_2O_2 by monitoring peroxidase-catalyzed oxidation of Amplex Red to resorufin (30). Mitochondria were isolated and resuspended with respiration buffer as described above for oxygen consumption. Mitochondria were then snap-frozen in liquid nitrogen and thawed four times for permeabilization. Mitochondrial samples at a final protein concentration of 400 μg/ml were supplemented with SOD1 (40 units/ml, Sigma-Aldrich), horseradish peroxidase (0.1 unit/ml, Molecular Probes), and Amplex Red (50 μM, Molecular Probes). The reaction mixture in Krebs-Ringer Phosphate (KRPG, 145 mM NaCl, 5.7 mM Na_2HPO_4, 4.86 mM KCl, 0.54 mM $CaCl_2$, 1.22 mM $MgSO_4$, and 5.5 mM glucose at pH 7.35) with or without 5 mM NADH or 5 mM succinate was incubated at 37 °C with readings every min at 544 nm excitation and 590 nm emission. Rates of NADH-driven electron flux through complex I were calculated over the linear increasing period, and the end plateau values of each reaction were treated as NADH- or succinate-induced mitochondrial ROS generation. For negative controls of basal activity, CAT (200 units/ml) was added at the beginning of the trace.

Immunoblotting—Mitochondrial isolation was performed as described above. Here, 10 mM triethanolamine and 0.1 mg/ml digitonin were added in mitochondria isolation buffer to weaken cell membrane. Resulting pellets were collected and resuspended with mitochondria buffer (250 mM sucrose, 10 mM Tris/HCl, and 0.2 mM EDTA at pH 7.8) supplemented with protease inhibitor mixture. For primary cells, 3 days after the 10-min oxidant exposure cell lysates were obtained and supplemented with protease inhibitor mixture.

Protein samples (10 μg/lane) were subjected to 10–20% SDS-PAGE gradient gel before transfer onto polyvinylidene fluoride membrane. Membrane was then blocked overnight at 4 °C with 3% (w/v) gelatin protein (Top Block, Juro, Switzerland) in mitochondria PBS (1.4 mM KH_2PO_4, 8 mM Na_2HPO_4, 140 mM NaCl, and 2.7 mM KCl at pH 7.3), incubated in mitochondria PBS containing 0.6% Top block with 0.05% Tween 20 and premixed mouse monoclonal antibodies against five subunits of oxidative phosphorylation complexes (MS604 1:250; MitoSciences, Eugene, OR) at room temperature for 2 h. After washing, the membrane was incubated with horseradish peroxidase-conjugated anti-mouse antibody (1:2000, Amersham Biosciences), and immunoreactivity was visualized by SuperSignal West Pico Chemiluminescent Substrate (Pierce) and Molecular Imager ChemiDoc XRS system (Bio-Rad).

Quantitative Real-time PCR—Total RNA from INS-1E cells and rat islets was extracted using the RNeasy Mini Kit (Qiagen) and TRIzol reagent (Invitrogen), respectively, according to the manufacturer's instructions. First-strand cDNA synthesis was performed with 2 μg of RNA, reverse transcriptase (Super Script II, Invitrogen), and 1 μg of random primers (Promega, Madison, WI) (32). Primers for NADH dehydrogenase 6 (*ND6*), cytochrome *c* oxidase I (*COX I*), mitochondrial transcription factor A (*TFAM*), peroxisome proliferator-activated receptor α coactivator 1 α (*PGC-1α*), copper/zinc (Cu/Zn)-dependent SOD (*SOD1*), manganese-dependent SOD (*SOD2*), catalase (*CAT*), glutathione peroxidase (*GPx*), uncoupling protein 2 (*UCP2*), were designed using the Primer Express Software (Applera Europe, Rotkreuz, Switzerland) and are listed in supplemental Table S1. Real-time PCR was performed using an ABI 7000 Sequence Detection System (Applera), and PCR products were quantified fluorometrically using the Power SYBR Green PCR Master Mix kit (Applied Biosystems). Values were normalized to the reference mRNA ribosomal protein subunit 29 (*RPS29*).

Mitochondrial Morphology—Mitochondria were revealed by MitoTracker Orange (Molecular Probes, Eugene, OR) staining on fixed cells. Briefly, after the mentioned recovery period following transient oxidative stress, cells on polyornithine-coated glass coverslips were washed with PBS twice and incubated with 100 nM MitoTracker at 37 °C for 25 min. After another wash, cells were fixed with 4% paraformaldehyde and washed extensively before mounting on glass slides. Cells were viewed using a confocal laser scanning 410 microscope (Carl Zeiss).

Statistical Analysis—Data are presented as the means ± S.E. unless otherwise indicated. One-way analysis of variance and two-tailed unpaired *t* test were used for statistical analysis. Results were considered statistically significant at $p < 0.05$.

RESULTS

INS-1E Cell Apoptosis and Proliferation Post-stress—Basal apoptotic rate in control INS-1E cells was ~2%, in agreement with previous observations (31). Single 10-min oxidative stress induced 20–25% TUNEL-positive cells 8-h post-stress, an apoptotic rate maintained throughout a 5-day period post-stress (Fig. 1*A*). INS-1E cells exhibited typical proliferation rate with 30% BrdUrd labeling (31), while oxidative stress transiently decreased cell proliferation 24 h post-injury (Fig. 1*B*). Five days later, stressed cells exhibited higher proliferation rate compared with naïve cells, the latter proliferating at a slower pace along with increasing cell to cell contacts favored by confluency (Fig. 1*B*). Representative pictures are shown in supplemental Fig. S3.

Insulin Secretion from INS-1E Cells 3 and 5 Days Post-stress—Insulin secretion from control INS-1E cells (Fig. 1*C*) evoked by 15 mM glucose was stimulated 4.8-fold *versus* control basal release ($p < 0.005$). Compared with controls, cells subjected to oxidative stress 3 days before experiments had a 110% increase in basal insulin release ($p < 0.05$) but did not respond to 15 mM glucose, corresponding to a 40% inhibition of the secretory response *versus* glucose-stimulated control cells ($p < 0.05$). Exocytosis evoked by 30 mM KCl, used to raise cytosolic Ca^{2+} independently of mitochondrial activation, was not different between the two groups. However, insulin release under basal conditions was elevated in stressed cells to levels comparable to KCl-induced responses of controls, therefore showing no further stimulation. Because it is known that, immediately after

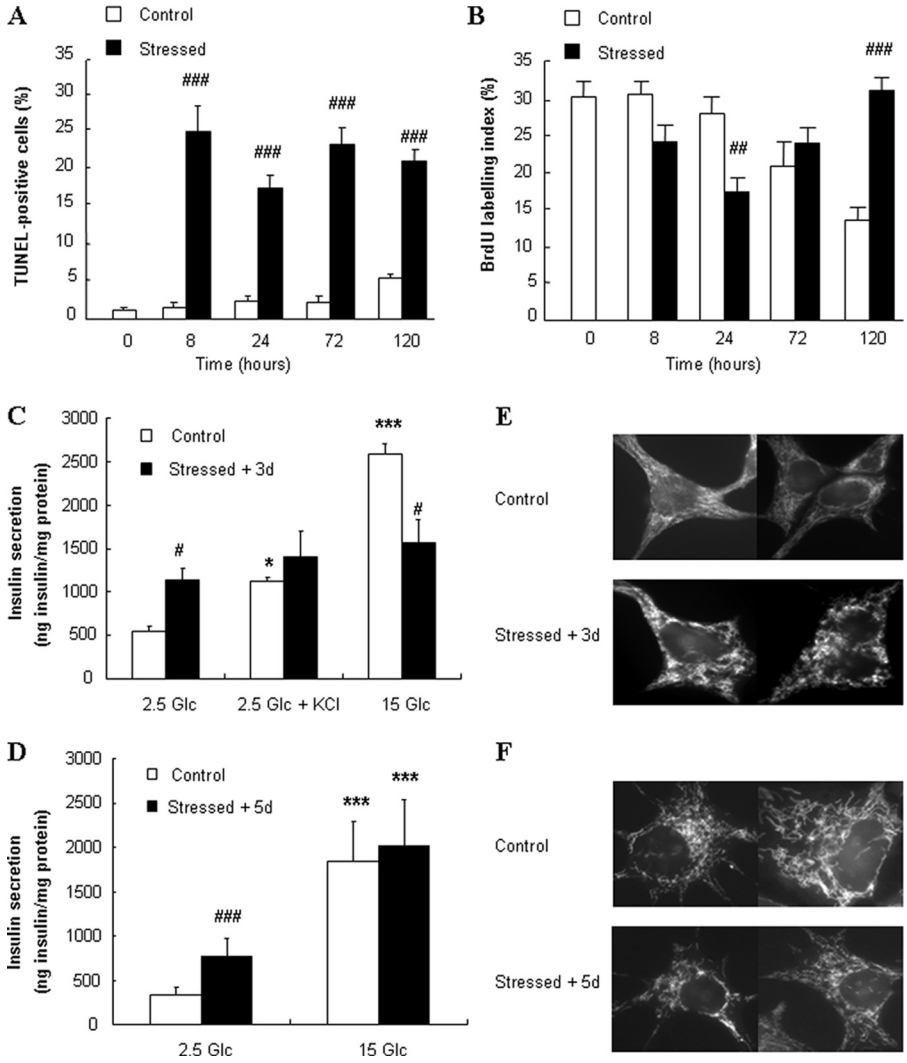

FIGURE 1. **Apoptosis/proliferation, secretory responses, and mitochondrial morphology of INS-1E cells during days following oxidative stress.** *A* and *B*, INS-1E cells were cultured for the indicated time points without stress (*Control*) or following transient oxidative stress (200 μM H_2O_2 for 10 min at time 0, *Stressed*). *A*, cell apoptosis and (*B*) proliferation were measured by the TUNEL assay and BrdUrd incorporation, respectively. TUNEL (*A*)- or BrdUrd (*B*)-positive cells were counted under fluorescent microscope in at least three separate fields (each containing ~70 cells) of four independent experiments, and graphical results are depicted as a percentage of positive cells over the total amount of insulin positive cells. *C* and *D*, insulin secretion tested in INS-1E cells cultured for 3 (*C*) and 5 (*D*) days following transient exposure to 200 μM H_2O_2 for 10 min (*Stressed + 3d* and *Stressed + 5d*) or without oxidative stress (*Control*). Insulin release was measured following a 30-min incubation at basal 2.5 mM glucose (*2.5 Glc*), stimulatory 15 mM glucose (*15 Glc*), and 2.5 Glc with 30 mM KCl (*2.5 Glc + KCl*). Values are means ± S.D. of 1 representative out of 5 different experiments performed in quintuplicate. *E* and *F*, visualization under laserscan confocal microscope of INS-1E cells stained for mitochondria using MitoTracker. 3 (*E*) and 5 (*F*) days after transient exposure to 200 μM H_2O_2 for 10 min (*Stressed + 3d* and *Stressed + 5d*) were compared with non-stressed cells (*Control*). Pictures shown are representative of three independent experiments. *, $p < 0.05$; ***, $p < 0.005$ *versus* basal secretion (2.5 Glc); #, $p < 0.05$; ##, $p < 0.01$; ###, $p < 0.005$ *versus* corresponding controls.

stress, H_2O_2 exposure raises Ca^{2+} to ~400 nM (12), we checked KCl responses in cells 3 days post-stress. Supplemental Fig. S4 shows efficient KCl-induced Ca^{2+} rise in stressed cells, suggesting impairment in the exocytotic machinery downstream of Ca^{2+} elevation.

Five days post-stress, we observed similar inhibition of the glucose response (2.1-fold *versus* 5.4-fold in stressed *versus* control conditions, respectively) associated with elevated basal insulin release (+127% *versus* control, $p < 0.005$; Fig. 1*D*). These data show that the single 10-min oxidative stress induced secretory defects lasting over days.

Mitochondrial Morphology in INS-1E Cells 3 and 5 Days Post-stress—To determine whether mitochondrial morphology was conserved after transient oxidant exposure, INS-1E mitochondrial shape was visualized (Fig. 1, *E* and *F*). Control cells exhibited normal filament-like mitochondria (Fig. 1, *E* and *F*, *top*), whereas exposure to 200 μM H_2O_2 3 days before observation resulted in discontinuous mitochondrial network, eventually presenting globular patterns (Fig. 1*E*, *bottom*). Mitochondrial morphology was restored 5 days after transient oxidative stress (Fig. 1*F*, *bottom*).

$\Delta\Psi_m$, ATP Levels, Complex I Activity and O_2 Consumption 3 Days Post-stress—Mitochondrial membrane was hyperpolarized when glucose was raised from 2.5 mM to 15 mM and depolarized by the subsequent addition of 1 μM of the protonophore FCCP (Fig. 2*A*). In INS-1E cells stressed 3 days before by 200 μM H_2O_2, glucose-induced mitochondrial hyperpolarization was inhibited by 55%, and total $\Delta\Psi_m$ revealed by FCCP was reduced by 42% compared with non-stressed controls (Fig. 2*A*). Exposure to 500 μM H_2O_2 resulted in near complete abrogation of glucose-induced hyperpolarization measured 3 days post-stress (supplemental Fig. S1).

Elevation of glucose from 2.5 mM to 15 mM in control cells resulted in a sustained elevation of cytosolic ATP levels (Fig. 2*B*), which were disrupted by adding the mitochondrial poison NaN_3. Stressed cells exhibited a 59% inhibition in glucose-induced ATP generation. Measured as absolute levels, total cellular ATP concentrations in control INS-1E cells stimulated with 15 mM glucose were increased by 31% ($p < 0.01$) compared with basal levels (Fig. 2*C*). Stressed cells exhibited lower basal (−42%, $p < 0.002$) and stimulated (−46%, $p < 0.0002$) ATP levels *versus* control cells.

Efficient electron transfer from NADH to complex I ensures activation of mitochondrial electron transport chain resulting in hyperpolarization of $\Delta\Psi_m$ and ATP generation. Electron transport chain complex I activity was measured using permeabilized isolated mitochondria as the rate of NADH-induced electron flux. INS-1E cells subjected to oxidative stress 3 days before analysis exhibited reduced mitochondrial complex I

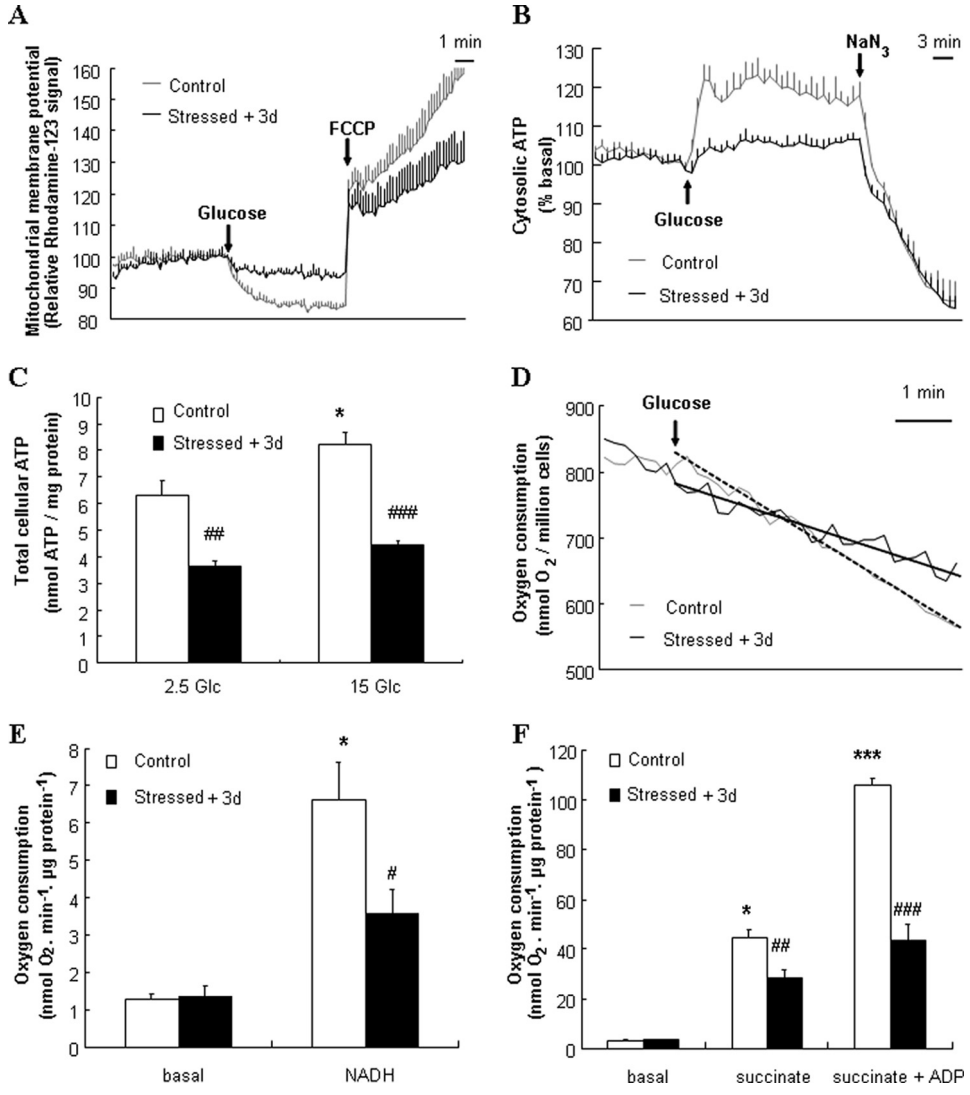

FIGURE 2. **Mitochondrial activation in INS-1E cells 3 days post-stress.** INS-1E cells were cultured for 3 days following transient oxidative stress (200 μM H_2O_2 for 10 min, *Stressed + 3d*) before analyses. *A*, $\Delta\Psi_m$ was monitored as Rhodamine-123 fluorescence and hyperpolarization was induced by raising glucose from basal 2.5 mM to stimulatory 15 mM (see *arrow*, *Glucose*). Complete depolarization of the mitochondrial membrane was evoked by addition of 1 μM of the uncoupler FCCP (see *arrow*, *FCCP*). *B*, real-time cytosolic ATP changes were monitored in luciferase expressing INS-1E cells as bioluminescence. ATP generation was induced by raising glucose from 2.5 to 15 mM (see *arrow*, *Glucose*) and collapsed by addition of the mitochondrial poison 2 mM NaN_3 (see *arrow*, *NaN_3*). *C*, total cellular ATP concentrations were determined following a 10-min incubation period at 2.5 (*2.5 Glc*) and 15 mM (*15 Glc*) glucose. Results are means ± S.D. of 1 representative out of 3 independent experiments, each performed in triplicate. *D*, O_2 consumption in INS-1E cells was induced by raising glucose from 0 to 15 mM (see *arrow*, *Glucose*). Tangents corresponding to glucose-induced respiration in control and stressed cells are shown as *dashed* and *dotted lines*, respectively. Traces are representative of four independent experiments. *E*, isolated mitochondria were permeabilized, placed into an oxymeter chamber, and stabilized for at least 10 min without substrates (*basal*). Then, complex I-dependent O_2 consumption was stimulated by the addition of 5 mM NADH (*NADH*). *F*, O_2 consumption was induced in intact mitochondria by adding 5 mM succinate (*succinate*), followed by further 150 μM ADP addition (*succinate + ADP*). *Columns* represent means ± S.E. of four independent experiments. *, $p < 0.01$; ***, $p < 0.001$ *versus* basal non-stressed controls; #, $p < 0.05$; ##, $p < 0.01$; and ###, $p < 0.005$ *versus* corresponding controls.

activity (−14%, $p < 0.001$, $n = 7$) compared with naïve cells (data not shown).

Measured in cell suspension, glucose-induced O_2 consumption rate was reduced in stressed cells compared with normal respiration in naïve cells (Fig. 2*D*). Measured in isolated mitochondria, basal respiratory rates were similar between control mitochondria and mitochondria isolated from cells transiently stressed with 200 μM H_2O_2 3 days before measurements. Complex I was activated by the addition of its substrate NADH (5 mM) to permeabilized mitochondria and resulted in a 5.1-fold ($p < 0.01$) increase in O_2 consumption in control mitochondria (Fig. 2*E*), which was totally abolished by the application of complex I inhibitor rotenone (data not shown). Compared with controls, mitochondria isolated from stressed cells showed a 43% ($p < 0.05$) reduction of the respiratory rate. Next, succinate was used as complex II substrate. In control mitochondria, state 4 respiration induced by 5 mM succinate and state 3 induced by further addition of 150 μM ADP resulted in 14.3- and 31.2-fold ($p < 0.01$ and $p < 0.001$, respectively) elevations of O_2 consumption, respectively (Fig. 2*F*). Transient exposure to oxidative stress 3 days prior to respiration measurements caused a decrease in both state 4 (−36%, $p < 0.01$) and state 3 (−59%, $p < 0.005$) respiration compared with corresponding controls. Concentrations of H_2O_2 lower than 200 μM (50 and 100 μM) did not alter O_2 consumption after 3 days (supplemental Fig. S2).

Mitochondrial Respiratory Chain Subunits in INS-1E Cells Post-stress—At this stage, data suggest that transient oxidative stress induced molecular modifications of mitochondrial machinery. By immunoblotting, we analyzed integrity of the mitochondrial respiratory chain complex subunits known to be preferentially lost as a result of mitochondrial damages (32). Three days after transient oxidative stress, the relative integrity of the five subunits was analyzed in mitochondria isolated from INS-1E β-cells (Fig. 3*A*). Densitometry analysis of four independent immunoblots showed that, compared with controls, transient exposure of INS-1E cells to H_2O_2 3 days before reduced levels of ND6 (complex I, −24%, $p < 0.01$), core2 (complex III, −21%, $p < 0.01$), and COX I (complex IV, −29%, $p < 0.01$) compared with non-stressed controls. A time course analysis revealed that loss of electron transport chain subunits was initiated as early as 6 h after H_2O_2 exposure for complexes I and III and immediately after oxidative stress for complex IV (Fig. 3*B*).

Expression of Mitochondrion-related Genes in INS-1E Cells 1–5 Days Post-stress—Next, expression of mitochondrion-associated genes was measured by quantitative reverse transcrip-

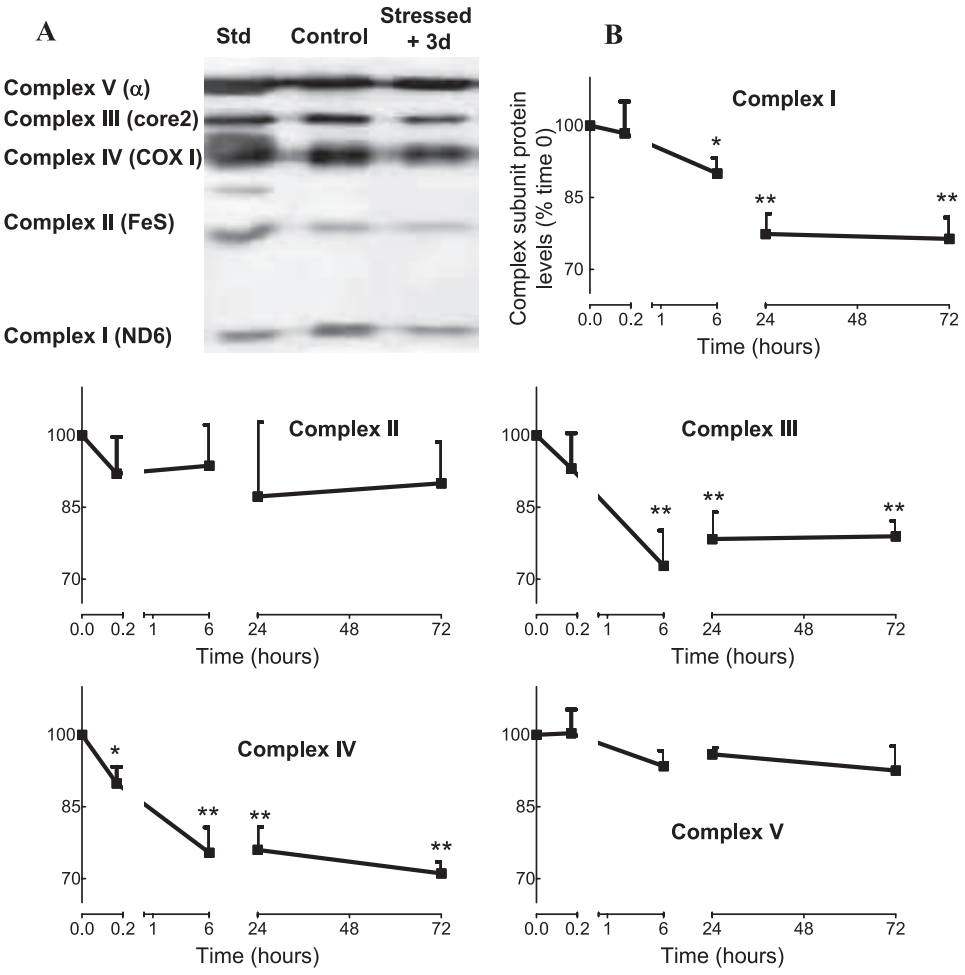

FIGURE 3. **Mitochondrial respiratory chain subunits in INS-1E cells over days post-stress.** INS-1E cells were subjected to transient oxidative stress (200 μM H_2O_2 for 10 min) and further cultured for recovery periods. Then, mitochondria were isolated for immunoblot analysis. *A*, representative immunoblotting revealing subunit proteins of the 5 complexes 3 days after transient oxidative stress. *Lanes* from *left* to *right* show standards (*Std*) for the five subunits (ND6 for complex I, FeS for complex II, COX I for complex IV, core2 for complex III, and α subunit for complex V), non-stressed INS-1E mitochondria (*Control*), and stressed mitochondria (*Stressed + 3d*). *B*, time course presenting subunit protein changes at times 0, 10 min, 6 h, 1 day, and 3 days after transient (10 min) exposure to 200 μM H_2O_2. Quantitative analysis of relative band densities (relative changes to time 0), as shown in *A*, is presented as means ± S.E. of four independent experiments; *, $p < 0.05$; **, $p < 0.01$ *versus* corresponding time 0.

tion-PCR: mtDNA-encoded electron transport chain complex subunits *ND6* and *COX I*; genes responsible for mitochondrial biogenesis, *TFAM* and *PGC-1α*; antioxidant enzymes *SOD1*, *SOD2*, *CAT*, and *GPx*; uncoupling protein, *UCP2* (Table 1). One day after oxidative stress, expression at the mRNA level was found to be up-regulated for *ND6* (+61%) and *COX I* (+76%), whereas at the protein levels these electron transport chain subunits were down-regulated (Fig. 3*B*). Three days after transient oxidant injury, mRNA of 7 of 9 genes tested were markedly modified in stressed cells compared with controls. In particular, there was an up-regulation of genes related to mitochondrial function (*ND6*, +31%; *COX I*, +61%) and detoxification (*SOD1*, +636%; *CAT*, +48%; and *UCP2*, +214%), whereas mitochondrial biogenesis related genes were down-regulated (*TFAM*, −24%; *PGC-1α*, −67%). No significant changes were observed in *SOD2* and *GPx* mRNA levels. Day-5 post-injury was associated with continuous up-regulation of genes associated to mitochondrial function (*ND6*, +205%; *COX I*, +133%) and detoxification (*SOD1*, +116%; *UCP2*, +169%), and down-regulation of mitochondrial biogenesis (*TFAM*, −37%; *PGC-1α*, −66%). These data suggest that rapid decline of electron transport chain subunits at the protein level induced up-regulation of corresponding gene expression.

Mitochondrial ROS Generation in INS-1E Cells 3 Days Post-stress—It has been shown that mitochondrial respiration chain dysfunction may be associated with increased ROS levels (17), suggesting that transient exogenous oxidative stress might favor endogenous ROS generation from altered mitochondria. To test this hypothesis, H_2O_2 production from INS-1E mitochondria was measured with mitochondrial electron donors NADH (5 mM) and succinate (5 mM). In control mitochondria, complex I-dependent NADH stimulation induced a 6.2-fold ($p < 0.001$) increase in ROS levels (Fig. 4*A*). The same stimulation applied on mitochondria isolated from stressed INS-1E cells caused a further increase in endogenous ROS production (+60%, $p < 0.05$). In response to the complex II substrate succinate, H_2O_2 generation in mitochondria from stressed cells increased by 40% ($p < 0.01$) compared with non-stressed group (Fig. 4*B*). As negative controls, CAT inhibited both NADH- and succinate-induced ROS accumulation.

Functionality of Rat Islets 3–5 Days Post-stress—Isolated rat pancreatic islets were cultured for 1 day before transient oxidative stress (200 μM H_2O_2) applied for 10 min. Non-stressed and stressed islets were allowed a further culture period in normal complete media before analyses. Visual inspection using conventional stereomicroscope did not reveal significant changes in islet morphology or necrosis 3 days after oxidative stress (data not shown).

For secretion assay, batches of 10 islets per chamber were perifused, first at basal 2.8 mM glucose, then at stimulatory 16.7 mM glucose for 30 min, and returned to basal for another 15 min period (Fig. 5*A*). Glucose-stimulated insulin secretion was markedly impaired in islets oxidatively stressed 3 days before experiments when compared with control islets (areas under the curve: 10.14 ± 6.58 *versus* 39.18 ± 8.56 ng insulin/10 islets over the 30-min stimulatory period, respectively, $p < 0.01$).

Three days after oxidative stress, part of islets batches were used for immunoblotting (Fig. 5*B*) using the same pre-mix antibody mixture as for INS-1E mitochondria (Fig. 3*A*). Similar to

TABLE 1

mRNA levels of mitochondrial related genes in INS-1E cells 1, 3, and 5 days after transient oxidative stress

Expression of target genes 1, 3, and 5 days after 10-min oxidant exposure was quantified, and their mRNA levels were normalized to those of RPS29. Results are means ± S.E. of three independent experiments done in triplicate. *p* values *versus* corresponding controls.

Time	Genes	Control	Stressed	*p*
1 day	*ND6*	0.23 ± 0.21	0.37 ± 0.26	<0.05
	COX I	0.62 ± 0.24	1.09 ± 0.26	<0.001
	TFAM	0.47 ± 0.24	0.46 ± 0.16	
	PGC-1α	0.24 ± 0.04	0.27 ± 0.08	
	UCP2	1.94 ± 0.30	2.19 ± 0.86	
3 days	*ND6*	0.36 ± 0.26	0.47 ± 0.24	<0.05
	COX I	0.59 ± 0.26	0.95 ± 0.30	<0.005
	TFAM	1.18 ± 0.25	0.90 ± 0.41	<0.01
	PGC-1α	1.45 ± 0.46	0.48 ± 0.20	<0.001
	SOD1	0.14 ± 0.09	1.03 ± 0.68	<0.005
	SOD2	1.31 ± 0.22	1.59 ± 0.35	
	CAT	0.63 ± 0.14	0.93 ± 0.13	<0.01
	GPx	0.89 ± 0.19	1.00 ± 0.06	
	UCP2	1.25 ± 0.26	3.93 ± 1.38	<0.01
5 days	*ND6*	1.33 ± 0.45	4.06 ± 1.86	<0.01
	COX I	0.97 ± 0.37	2.26 ± 0.59	<0.005
	TFAM	0.76 ± 0.18	0.48 ± 0.20	<0.05
	PGC-1α	0.68 ± 0.28	0.23 ± 0.02	<0.05
	SOD1	0.38 ± 0.13	0.82 ± 0.44	<0.001
	SOD2	0.68 ± 0.36	0.86 ± 0.15	
	CAT	0.86 ± 0.09	0.70 ± 0.16	
	GPx	0.79 ± 0.18	0.79 ± 0.19	
	UCP2	1.21 ± 0.29	3.25 ± 0.36	<0.005

data obtained using INS-1E cells, stressed islets exhibited reduced levels of subunits ND6 (complex I), FeS (complex II), and core2 (complex III) compared with control islets (Fig. 5*B*).

Three and five days post-stress, mitochondrion-associated gene expression profile was determined in rat islets (Table 2). Three days post-injury, mRNA levels of antioxidants were increased in stressed islets compared with controls (*CAT*, +55%; *GPx*, +51%). Day 5 post-injury was also associated with changes of antioxidants (*CAT*, +58%; *SOD1*, −48%; *SOD2*, −61%) and mitochondrial biogenic factor (*TFAM*, −51%). These data show similar responses between INS-1E cells and primary islets in terms of antioxidant defenses, although repair mechanisms of mitochondrial electron transport chain subunits seem to be less efficient in islets.

Recovery of Islet and INS-1E Functions over Weeks—We then examined if oxidative stressed-induced dysfunction was reversible over longer (2–4 weeks) recovery periods. Following a recovery period of 3 weeks post-stress in normal culture condition, stressed islets exhibited full recovery of secretory responses to glucose (Fig. 6*A*), because we observed no differences in both basal insulin release at 2.8 mM glucose and in secretion evoked by 16.7 mM glucose (4.5- and 3.7-fold increases in control and stressed islets, respectively).

In INS-1E cells, O_2 consumption rate (Fig. 6*B*), testing efficiency of the mitochondrial machinery, was measured 2, 3, and 4 weeks after the acute 10-min exposure to 200 μM H_2O_2 with isolated mitochondria. During this recovery period, control and stressed cells were cultured as usual. Compared with the impaired respiratory function measured 3 days after the oxidative stress, INS-1E mitochondrial state 3 respiration was slightly improved (+32%, $p < 0.01$) following a recovery period of 2 weeks. However, compared with non-stressed controls, both state 4 and state 3 were still inhibited (−22%, $p < 0.05$ and −27%, $p < 0.05$) in these mitochondria. After 3 and 4 weeks, no

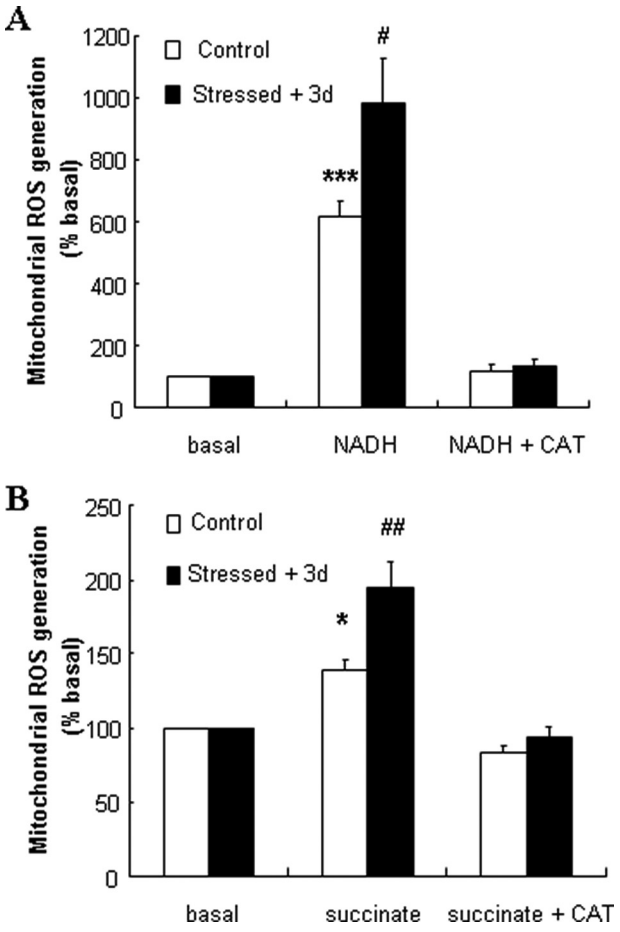

FIGURE 4. **ROS generation in INS-1E cells over days post-stress.** INS-1E cells were subjected to transient oxidative stress (200 μM H_2O_2 for 10 min) and further cultured for recovery periods. Then, mitochondria were isolated for endogenous ROS generation. *A* and *B*, 3 days after transient exposure to exogenous ROS, mitochondrion-derived ROS generation was measured in the absence of electron donors (*basal*) or induced by treatments with (*A*) 5 mM NADH (NADH) and (*B*) 5 mM succinate (*succinate*). CAT (200 units/ml) was added in the assay to obtain values corresponding to negative controls (NADH + CAT in *A* or succinate + CAT in *B*). *Columns* represent relative increases over non-stimulated groups as means ± S.E. of five independent determinations; *, $p < 0.05$; ***, $p < 0.005$ *versus* basal ROS generation in non-stressed control mitochondria; #, $p < 0.05$; ##, $p < 0.01$ *versus* corresponding controls.

significant differences were observed in both respiration states 4 and 3 *versus* corresponding non-stressed control conditions, indicating complete recovery of mitochondrial function.

Glucose-stimulated insulin secretion in INS-1E cells was tested following a recovery period of 2 and 3 weeks post-stress. After 2 weeks post-injury, stressed cells maintained elevated basal insulin release (+43%, $p < 0.05$), and attenuated glucose response (5.1- and 3.3-fold in control and 2 weeks post-stress, respectively, $p < 0.05$, Fig. 6*C*). Consistent with O_2 consumption rate, secretory function totally recovered 3 weeks post-stress as both basal insulin release at 2.5 mM glucose and secretory response to 15 mM glucose were similar to controls (Fig. 6*E*).

Mitochondrial morphology also recovered, showing no significant differences between control and stressed conditions 2 and 3 weeks post-stress (Fig. 6, *D* and *F*, respectively). The data show that persistent β-cell dysfunction observed 3 days after oxidative injuries was not associated to permanent impairment.

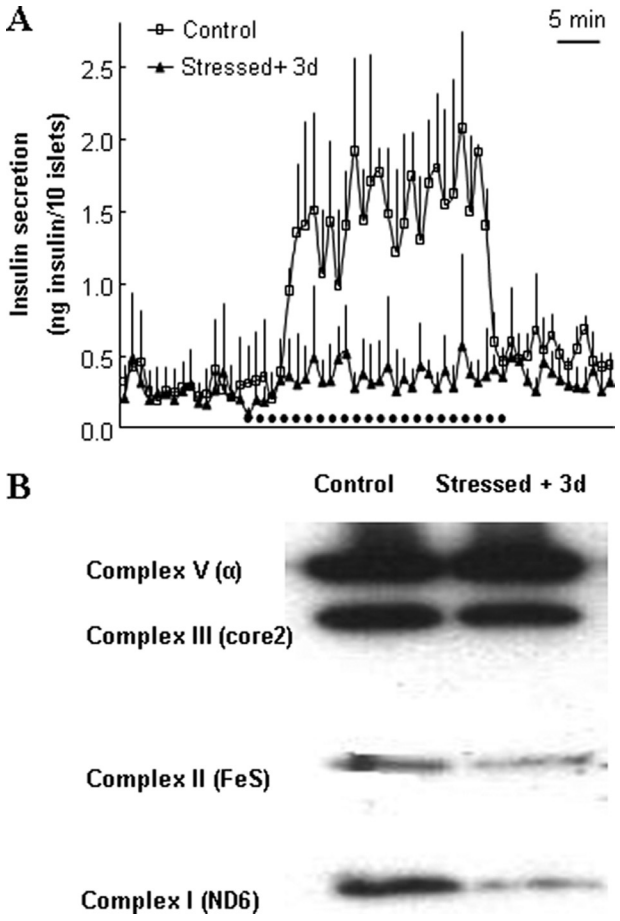

FIGURE 5. **Functionality of rat islets 3 days post-stress.** Isolated rat islets were transiently stressed with 200 μM H_2O_2 for 10 min and further maintained in culture for 3 days before analyses. *A*, insulin secretion was assayed by perifusion (10 islets per chamber) in islets stimulated with 16.7 mM glucose for 30 min (*horizontal dotted trace*) after 15 min at basal 2.8 mM glucose and then back to basal glucose for another 15 min. *Traces* are means ± S.D. of three chambers of one out of four individual experiments, each performed in triplicate. *B*, representative immunoblotting showing levels of the mitochondrial complex subunits (*I*, *II*, *III*, and *V*) of rat islets stressed 3 days before analysis.

TABLE 2

mRNA levels of mitochondrial related genes in rat islets 3 and 5 days after transient oxidative stress

Expression of target genes 3 and 5 days after 10-min oxidant exposure was quantified, and their mRNA levels were normalized to those of RPS29. Results are means ± S.E. of three independent experiments done in triplicate. *p* values *versus* corresponding controls.

Time	Genes	Control	Stressed	*p*
3 days	*ND6*	1.17 ± 0.04	1.12 ± 0.05	
	COX I	0.88 ± 0.04	0.93 ± 0.05	
	TFAM	1.08 ± 0.05	1.13 ± 0.07	
	PGC-1α	0.55 ± 0.16	0.53 ± 0.03	
	SOD1	1.64 ± 0.13	1.51 ± 0.11	
	SOD2	1.22 ± 0.05	1.24 ± 0.03	
	CAT	0.93 ± 0.13	1.44 ± 0.15	<0.01
	GPx	0.90 ± 0.05	1.36 ± 0.06	<0.01
	UCP2	0.81 ± 0.03	0.74 ± 0.02	
5 days	*ND6*	1.70 ± 0.14	1.92 ± 0.09	
	COX I	1.25 ± 0.07	1.24 ± 0.06	
	TFAM	0.95 ± 0.04	0.47 ± 0.11	<0.01
	PGC-1α	0.70 ± 0.02	0.53 ± 0.05	
	SOD1	0.82 ± 0.06	0.43 ± 0.04	<0.005
	SOD2	2.13 ± 0.04	0.84 ± 0.24	<0.005
	CAT	0.71 ± 0.05	1.12 ± 0.17	<0.05
	GPx	0.74 ± 0.05	0.77 ± 0.11	
	UCP2	1.12 ± 0.04	1.16 ± 0.05	

Gene Expression Profile after a 3-Week Recovery Period in INS-1E Cells—Three days after oxidative stress, while mitochondrial function was severely impaired, we observed an up-regulation of genes related to mitochondrial function and detoxification and down-regulation of genes responsible for mitochondrial biogenesis (Table 1). Three weeks after oxidative stress, mitochondrial and secretory functions were recovered (Fig. 6). Gene expression profile was then examined at this time point (Table 3). Among genes analyzed, only *UCP2* expression was still modified (+78%, $p < 0.05$) in INS-1E cells injured 3 weeks before compared with naïve cells.

Sensitivity of Recovered INS-1E Cells to a Second Oxidative Stress—Three weeks after transient oxidative stress, we then tested the sensitivity of INS-1E cells stressed 3 weeks prior to a second acute exposure to 200 μM H_2O_2 by monitoring cell apoptosis, proliferation, glucose-induced insulin secretion, and $\Delta\Psi_m$ (Fig. 7). In both naïve and recovered cells, 8 h after secondary 10-min stress, similar percentage of TUNEL-positive (Fig. 7*A*) and BrdUrd labeled (Fig. 7*B*) cells were observed, consistent with apoptotic and proliferation rate detected 8 h after the primary injury (Fig. 1, *A* and *B*). Insulin secretory responses were also similar to the one observed 3 days after the primary stress, *i.e.* elevated basal release and blunted glucose-stimulated insulin secretion (Fig. 7*C*). However, differences in glucose-induced mitochondrial activation were recorded after the second stress (Fig. 7*D*). In both naïve and recovered cells, mitochondrial membrane was hyperpolarized as expected upon glucose stimulation and depolarized by the addition of 1 μM of the protonophore FCCP. Application of 200 μM H_2O_2 for 10 min (at 2.5 mM glucose) to both naïve and recovered cells resulted in rapid depolarization of $\Delta\Psi_m$, in agreement with previous observations (12). Then, glucose was raised directly after this 10-min stress. Compared with control naïve cells, H_2O_2-induced mitochondrial depolarization was somewhat limited by the compensatory glucose-induced hyperpolarization in recovered cells, showing partial protection against oxidative stress (24%, $p < 0.001$) at the mitochondrial level.

DISCUSSION

Efficient mitochondrial function is essential for nutrient-induced insulin secretion from pancreatic β-cells. However, mitochondrial activation also gives rise to ROS generation that might be detrimental for β-cell function and survival (24).

In the present study, we observed mitochondrial damages after a 3-day recovery period following an acute 10-min exposure to H_2O_2. Transient exposure to primary exogenous ROS resulted in subsequent generation of secondary endogenous ROS of mitochondrial origin. These data suggest adaptive effects at mitochondrial level induced by oxidative stress. Previous studies typically analyzed cell function during and immediately following oxidative attacks (12, 25, 33). Here, we observed persistent alterations of β-cell function resulting in elevated basal insulin release and severely impaired glucose-stimulated insulin secretion. This is consistent with the observed mitochondrial damages, resulting in impaired metabolism-secretion coupling. Downstream of mitochondria, the secretory machinery might be affected as well by oxidative stress, because the secretory response to KCl was also inhibited.

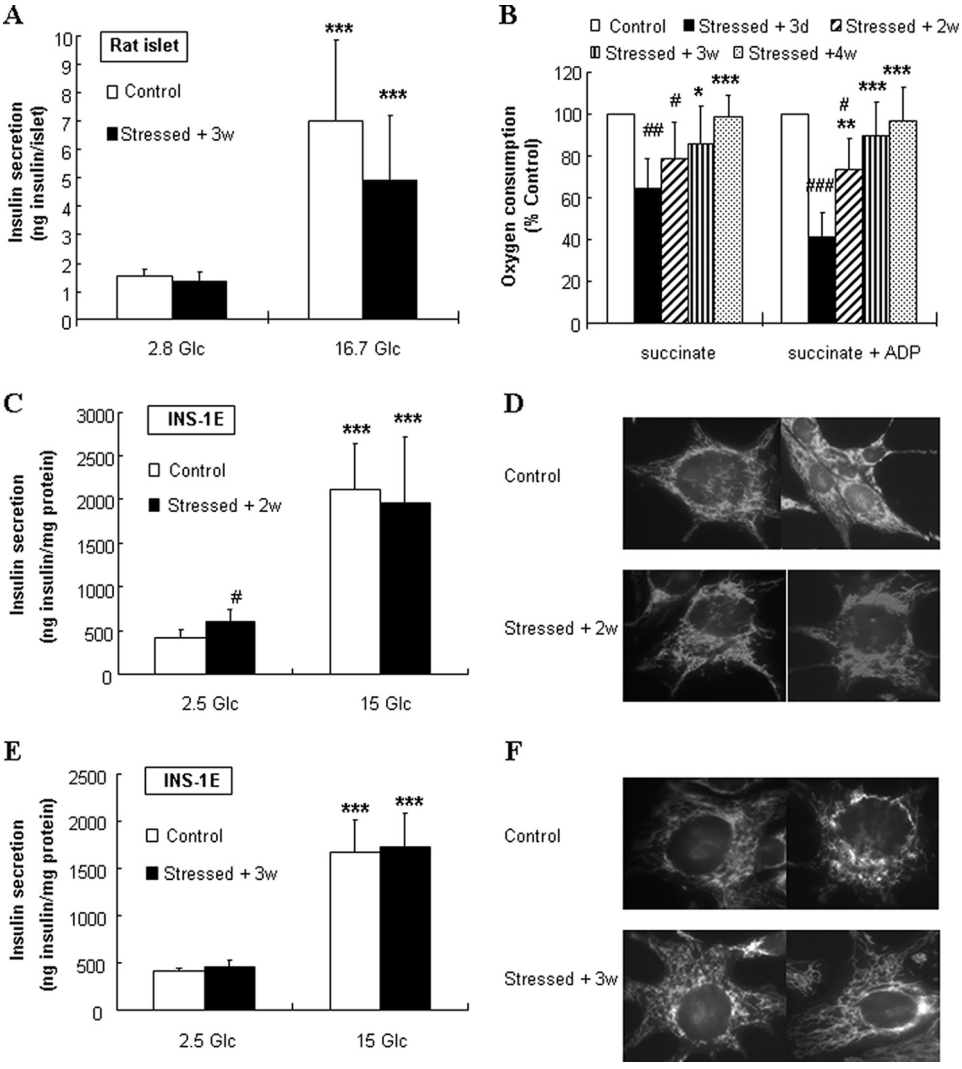

FIGURE 6. **Recovery of islet function, INS-1E secretory responses, and mitochondrial integrity.** Following transient oxidative stress (200 μM H_2O_2 for 10 min), rat islets and INS-1E cells were cultured for recovery periods of 2, 3, and 4 weeks before analyses. Stressed cells (*Stressed + 2w*, *3w*, and *4w*, respectively) were compared with cells stressed 3 days before (*Stressed + 3d*) and to non-stressed cells (*Control*). *A*, insulin secretion was measured over a 60-min incubation period at basal 2.8 mM glucose (*2.8 Glc*) and stimulatory 16.7 mM glucose (*16.7 Glc*) in rat islets cultured in normal media for 3 weeks following transient oxidative stress. *B*, mitochondria were isolated from INS-1E cells for respiratory rate measurements. O_2 consumption was induced by 5 mM succinate (*succinate*) and succinate plus 150 μM ADP (*succinate + ADP*). O_2 consumption is expressed as stimulated rates relative to corresponding non-stressed controls. *Bars* represent means ± S.E. of five independent measurements; *, $p < 0.05$; **, $p < 0.01$; and ***, $p < 0.005$ *versus* corresponding 3 days post-stress; #, $p < 0.05$; ##, $p < 0.01$; and ###, $p < 0.005$ *versus* corresponding controls. 2 (*C*) and 3 (*E*) weeks following transient oxidative stress or without oxidative stress, secretory function was tested in INS-1E cells by measuring glucose-stimulated insulin secretion. Basal insulin release at 2.5 mM basal glucose (*2.5 Glc*) was compared with stimulated secretion at 15 mM glucose (*15 Glc*) Values are means ± S.D. of one representative out of three different experiments performed in triplicate. *D* and *F*, visualization of mitochondria by confocal microscopy of INS-1E cells stained with MitoTracker. 2 (*D*) and 3 (*F*) weeks after transient exposure to 200 μM H_2O_2 for 10 min. ***, $p < 0.005$ *versus* basal secretion (*A*, 2.8 Glc; *C* and *E*, 2.5 Glc); #, $p < 0.05$ *versus* corresponding controls.

TABLE 3

mRNA levels of mitochondrial related genes in INS-1E cells after recovery

After recovery, mRNA levels of target genes were quantified and normalized. Results are means ± S.E. of three independent experiments done in triplicate. *p* values *versus* corresponding controls.

Genes	Control	Stressed (3 weeks)	*p*
TFAM	0.50 ± 0.13	0.84 ± 0.23	
PGC-1α	0.26 ± 0.09	0.23 ± 0.09	
SOD1	0.59 ± 0.17	0.46 ± 0.07	
SOD2	0.67 ± 0.29	0.51 ± 0.11	
CAT	0.24 ± 0.06	0.24 ± 0.05	
GPx	0.43 ± 0.09	0.60 ± 0.20	
UCP2	0.72 ± 0.14	1.28 ± 0.14	<0.05

Sub-lethal oxidative damages have been shown to induce endogenous ROS production in several cell types (34–36). Consistent with this concept, our data showed higher mitochondrial ROS production in INS-1E β-cells following exposure to exogenous oxidative stress. Subsequent endogenous ROS generation might contribute to prolongation of oxidative damages, correlating with reduction of respiratory chain complex proteins detected over a period of 3 days after stress. Previous studies reported that ROS production is associated with electron transport chain inhibition and mtDNA mutations (17, 37, 38). Accordingly, blockade of the respiratory chain allows electrons to be transferred directly to molecular oxygen to form superoxide (39). Therefore, previous and present results suggest breakdown of electron transport chain complexes as candidate mechanism for subsequent mitochondrial ROS generation. Other stressors than a primary oxidative stress have been shown to exert detrimental effects on mitochondria (40–42), raising the possibility of common mechanisms related to secondary endogenous ROS generation from damaged mitochondria.

In INS-1E cells, apoptotic rate was ~20–25% from 8 h until 5 days post-stress. Persistence of apoptosis could result from subsequent endogenous ROS generation observed after 3 days. When using the proliferating INS-1E preparation, cells analyzed 3 days after the primary insult were daughter cells of those which survived H_2O_2 exposure. This means that primary mitochondrial defects were carried on to the next generations, possibly with the contribution of additional damages provoked by endogenous ROS. Noteworthy, a similar degree of mitochondrial damages was recorded in the non-dividing primary islet cells. This suggests that near absence of cell division was not an aggravating factor regarding cell function.

INS-1E dysfunction was associated with induction of recovery mechanisms through up-regulation of genes responsible for mitochondrial function and detoxification. In particular, there was increased expression of antioxidants *SOD1* and *CAT*, and activation of *UCP2*, reducing potential oxidative damages

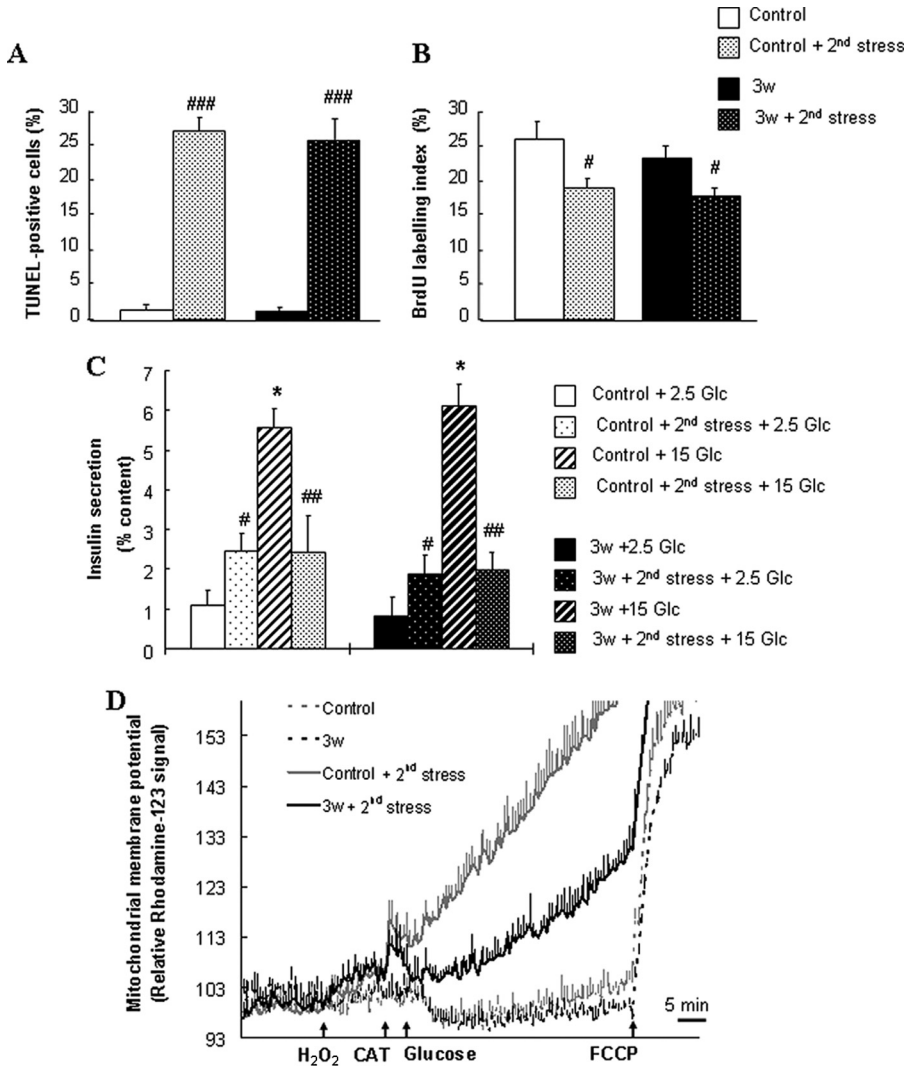

FIGURE 7. **Sensitivity of recovered INS-1E cells to a second oxidative stress.** After 3 weeks of recovery post-stress, cells were exposed for a second time to the same oxidative attack of 200 μM H_2O_2 for 10 min. Stressed cells allowed recovery period (*Stressed + 3w*) were compared with naïve cells (*Control*) for responses to a new oxidative stress (*Control + 2nd stress* and *Stressed + 2nd stress*). Cell apoptosis (*A*) and proliferation (*B*) were measured by the TUNEL assay and BrdUrd incorporation, respectively, as described in the legend of Fig. 1. *C*, insulin secretion tested in INS-1E cells cultured for 3 weeks following transient exposure to 200 μM H_2O_2 for 10 min or without oxidative stress. Directly after the second oxidative stress, insulin release was measured at basal 2.5 mM (*2.5 Glc*) and stimulatory 15 mM glucose (*15 Glc*). Values are means ± S.D. of one representative out of four different experiments performed in triplicate. *D*, mitochondrial activation was measured as changes in $\Delta\Psi_m$ induced by raising glucose from basal 2.5 mM to stimulatory 15 mM (see *arrow*, *Glucose*), and complete depolarization of the mitochondrial membrane was evoked by addition of 1 μM of the uncoupler FCCP (see *arrow*, *FCCP*). The 10-min 200 μM H_2O_2 stress was performed at basal 2.5 mM glucose (H_2O_2), and then 15 mM glucose stimulation was done after neutralization of H_2O_2 by adding 100 units/ml CAT. *Bars* are means ± S.D. of one out of four independent experiments, each performed in triplicate.

cross-talk resulting in slow-down of mitochondrial biogenesis specifically while repair mechanisms were induced to recover the function of existing mitochondria.

INS-1E cells could ultimately recover following a 3-week culture period after the 10-min oxidative stress, showing that damages were persistent but not permanent, at least in proliferating cells. Cells, tested 3 weeks after oxidative stress, are daughter cells of the ones analyzed at day 3. Remarkably, 3 weeks after oxidative stress these INS-1E cells responded normally to physiological stimuli but were more resistant than naïve cells to a second exogenous oxidative stress, showing again long-term persistence of the primary oxidative attack. This beneficial "memory" correlated with higher *UCP2* expression, in accordance with protective effects of UCP2 against ROS as discussed above (45).

Activation of mitochondria relies on functional complexes of the electron transport chain. These complexes ensure (i) efficient transport of electrons from complexes I and II then to oxygen through complexes III and IV, (ii) translocation of protons across the inner mitochondrial membrane, and (iii) ATP production at the expense of $\Delta\Psi_m$. Any alterations of these complex's components may result in mitochondrial dysfunction. Reduction of respiratory chain complex subunits possibly contributed to the observed persistent effect induced by transient oxidative stress. Noteworthy, subunits of complexes I, III, and IV were more sensitive than those of complexes II and V. Subunit sensitivity might be associated with their respective proximity to ROS sources, in particular regarding complexes directly responsible for ROS generation (13). Therefore, oxidative stress might have induced direct degradation of the subunits. An alternative mechanism could be reduced expression at transcriptional or post-transcriptional levels, which turned out to be unlikely. Indeed, loss of electron transport chain subunits could not be explained by reduced expression of corresponding genes, because transcript levels of *ND6* (complex I) and *COX I* (complex III) were up-regulated following oxidative stress, possibly as compensatory responses. Oxidative stress might induce ER stress that would affect subunit expression at the post-transcriptional levels. The β-cells through decrease of proton motive force. A protective role for UCP2 being activated by ROS was primarily documented in neurons and cardiomyocytes (43, 44) and further substantiated by a recent study showing that elevated UCP2 levels decrease cytokine-induced production of ROS in INS-1 β-cells (45).

Although some genes encoding antioxidant proteins were up-regulated, there was down-regulation of *TFAM* and *PGC-1α*. Thus, expression of nuclear genome-encoded genes participating to mitochondrial biogenesis (*TFAM* and *PGC-1α*) was halted 3 days post-stress but re-activated after 3 weeks. As naïve and stressed cells proliferated similarly at both time points post-stress, this raises the possibility of mitochondrion-nucleus

have a highly developed and active ER that provides a specialized environment for post-transcriptional modifications (46). ER stress has been shown to contribute to alterations in β-cell function and induction of ROS production, leading to prolonged oxidative stress (47, 48). Here, measurements of three classic β-cell ER stress markers 6 and 12 h after transient oxidant attack showed no evidence of ER stress (see supplemental Tables S2 and S3). Therefore, mitochondrial protein damage, rather than being a stochastic phenomenon, is likely to be an immediate and early consequence of ROS attack. To overcome injured respiratory chain complexes, post-stress compensatory responses are induced to restore impaired mitochondrial subunits through up-regulation of transcription.

In conclusion, our results demonstrate that one single transient oxidative stress durably impacts on β-cells over days and weeks, first, through persistent mitochondrial dysfunction and generation of endogenous ROS production, thereby contributing to a vicious cycle that prolongs the oxidative attack; and second, through induction of repair mechanisms that enable the injured mitochondria to ultimately recover and to become even more resistant to a new oxidative attack. These data indicate that the basic components of the mitochondrial theory of aging must be viewed in the context of different layers of complexity. These include both the nature and duration of the oxidative stress, the antioxidant defenses present in the target cell and a delicate balance between self-perpetuating and repair mechanisms.

REFERENCES

1. Maechler, P. (2002) *Cell Mol. Life Sci.* **59,** 1803–1818
2. Green, K., Brand, M. D., and Murphy, M. P. (2004) *Diabetes* **53,** Suppl. 1, S110–S118
3. Yu, B. P. (1994) *Physiol. Rev.* **74,** 139–162
4. Rabinovitch, A. (1998) *Diabetes Metab. Rev.* **14,** 129–151
5. Evans, J. L., Goldfine, I. D., Maddux, B. A., and Grodsky, G. M. (2002) *Endocr. Rev.* **23,** 599–622
6. Robertson, R. P., Harmon, J., Tran, P. O., Tanaka, Y., and Takahashi, H. (2003) *Diabetes* **52,** 581–587
7. Mandrup-Poulsen, T. (2001) *Diabetes* **50,** Suppl. 1, S58–S63
8. Rhee, S. G. (2006) *Science* **312,** 1882–1883
9. Pi, J., Bai, Y., Zhang, Q., Wong, V., Floering, L. M., Daniel, K., Reece, J. M., Deeney, J. T., Andersen, M. E., Corkey, B. E., and Collins, S. (2007) *Diabetes* **56,** 1783–1791
10. Tiedge, M., Lortz, S., Drinkgern, J., and Lenzen, S. (1997) *Diabetes* **46,** 1733–1742
11. Welsh, N., Margulis, B., Borg, L. A., Wiklund, H. J., Saldeen, J., Flodström, M., Mello, M. A., Andersson, A., Pipeleers, D. G., and Hellerström, C. (1995) *Mol. Med.* **1,** 806–820
12. Maechler, P., Jornot, L., and Wollheim, C. B. (1999) *J. Biol. Chem.* **274,** 27905–27913
13. Turrens, J. F. (2003) *J. Physiol.* **552,** 335–344
14. Li, N., Frigerio, F., and Maechler, P. (2008) *Biochem. Soc Trans.* **36,** 930–934
15. Maechler, P., and de Andrade, P. B. (2006) *Biochem. Soc Trans.* **34,** 824–827
16. Wallace, D. C. (1999) *Science* **283,** 1482–1488
17. de Andrade, P. B., Rubi, B., Frigerio, F., van den Ouweland, J. M., Maassen, J. A., and Maechler, P. (2006) *Diabetologia* **49,** 1816–1826
18. Trifunovic, A., Hansson, A., Wredenberg, A., Rovio, A. T., Dufour, E., Khvorostov, I., Spelbrink, J. N., Wibom, R., Jacobs, H. T., and Larsson, N. G. (2005) *Proc. Natl. Acad. Sci. U.S.A.* **102,** 17993–17998
19. Bua, E., Johnson, J., Herbst, A., Delong, B., McKenzie, D., Salamat, S., and Aiken, J. M. (2006) *Am. J. Hum. Genet.* **79,** 469–480
20. Shigenaga, M. K., Hagen, T. M., and Ames, B. N. (1994) *Proc. Natl. Acad. Sci. U.S.A.* **91,** 10771–10778
21. Harman, D. (1956) *J. Gerontol.* **11,** 298–300
22. Cottrell, D. A., and Turnbull, D. M. (2000) *Curr. Opin. Clin. Nutr. Metab. Care* **3,** 473–478
23. Simmons, R. A., Suponitsky-Kroyter, I., and Selak, M. A. (2005) *J. Biol. Chem.* **280,** 28785–28791
24. Bindokas, V. P., Kuznetsov, A., Sreenan, S., Polonsky, K. S., Roe, M. W., and Philipson, L. H. (2003) *J. Biol. Chem.* **278,** 9796–9801
25. Krippeit-Drews, P., Kramer, C., Welker, S., Lang, F., Ammon, H. P., and Drews, G. (1999) *J. Physiol.* **514,** 471–481
26. Merglen, A., Theander, S., Rubi, B., Chaffard, G., Wollheim, C. B., and Maechler, P. (2004) *Endocrinology* **145,** 667–678
27. Carobbio, S., Ishihara, H., Fernandez-Pascual, S., Bartley, C., Martin-Del-Rio, R., and Maechler, P. (2004) *Diabetologia* **47,** 266–276
28. Ishihara, H., Maechler, P., Gjinovci, A., Herrera, P. L., and Wollheim, C. B. (2003) *Nat. Cell Biol.* **5,** 330–335
29. Maechler, P., Wang, H., and Wollheim, C. B. (1998) *FEBS Lett.* **422,** 328–332
30. Keeney, P. M., Xie, J., Capaldi, R. A., and Bennett, J. P., Jr. (2006) *J. Neurosci.* **26,** 5256–5264
31. Brun, T., Duhamel, D. L., Hu He, K. H., Wollheim, C. B., and Gauthier, B. R. (2007) *Oncogene* **26,** 4261–4271
32. Boengler, K., Gres, P., Dodoni, G., Konietzka, I., Di Lisa, F., Heusch, G., and Schulz, R. (2007) *J. Mol. Cell Cardiol.* **43,** 610–615
33. Janjic, D., Maechler, P., Sekine, N., Bartley, C., Annen, A. S., and Wolheim, C. B. (1999) *Biochem. Pharmacol.* **57,** 639–648
34. Seshiah, P. N., Weber, D. S., Rocic, P., Valppu, L., Taniyama, Y., and Griendling, K. K. (2002) *Circ. Res.* **91,** 406–413
35. Li, W. G., Miller, F. J., Jr., Zhang, H. J., Spitz, D. R., Oberley, L. W., and Weintraub, N. L. (2001) *J. Biol. Chem.* **276,** 29251–29256
36. Tampo, Y., Kotamraju, S., Chitambar, C. R., Kalivendi, S. V., Keszler, A., Joseph, J., and Kalyanaraman, B. (2003) *Circ. Res.* **92,** 56–63
37. Barrientos, A., and Moraes, C. T. (1999) *J. Biol. Chem.* **274,** 16188–16197
38. Esposito, L. A., Melov, S., Panov, A., Cottrell, B. A., and Wallace, D. C. (1999) *Proc. Natl. Acad. Sci. U.S.A.* **96,** 4820–4825
39. Delgado, E. H., Streck, E. L., Quevedo, J. L., and Dal-Pizzol, F. (2006) *Neurochem. Res.* **31,** 1021–1025
40. Eizirik, D. L., Strandell, E., Bendtzen, K., and Sandler, S. (1988) *Diabetes* **37,** 916–919
41. Moreira, J. E., Hand, A. R., Håkan Borg, L. A., Sandler, S., Welsh, M., Welsh, N., and Eizirik, D. L. (1991) *Virchows Arch. B Cell Pathol. Incl. Mol. Pathol.* **60,** 337–344
42. Sandler, S., Bendtzen, K., Borg, L. A., Eizirik, D. L., Strandell, E., and Welsh, N. (1989) *Endocrinology* **124,** 1492–1501
43. Mattiasson, G., Shamloo, M., Gido, G., Mathi, K., Tomasevic, G., Yi, S., Warden, C. H., Castilho, R. F., Melcher, T., Gonzalez-Zulueta, M., Nikolich, K., and Wieloch, T. (2003) *Nat. Med.* **9,** 1062–1068
44. Teshima, Y., Akao, M., Jones, S. P., and Marbán, E. (2003) *Circ. Res.* **93,** 192–200
45. Produit-Zengaffinen, N., Davis-Lameloise, N., Perreten, H., Bécard, D., Gjinovci, A., Keller, P. A., Wollheim, C. B., Herrera, P., Muzzin, P., and Assimacopoulos-Jeannet, F. (2007) *Diabetologia* **50,** 84–93
46. Eizirik, D. L., Cardozo, A. K., and Cnop, M. (2008) *Endocr. Rev.* **29,** 42–61
47. Oyadomari, S., Koizumi, A., Takeda, K., Gotoh, T., Akira, S., Araki, E., and Mori, M. (2002) *J. Clin. Invest.* **109,** 525–532
48. Kitiphongspattana, K., Khan, T. A., Ishii-Schrade, K., Roe, M. W., Philipson, L. H., and Gaskins, H. R. (2007) *Am. J. Physiol. Endocrinol. Metab.* **292,** E1543–E1554